Vision-Based Cooperative Simultaneous Localization and Tracking

Chun-Hua Chang, Shao-Chen Wang and Chieh-Chih Wang

***Abstract*— Localization is one of the most essential capabilities of autonomous robots. Cooperative localization has been proved to be effective in multi-robot localization. However, nearby moving objects could degrade the cooperative localization performance. In this paper, we demonstrate that the cooperative simultaneous localization and tracking approach is superior in challenging scenarios. Localization and moving object tracking are mutually beneficial. The proposed approach is evaluated using humanoid robots in the RoboCup environment in which only uncertain data from onboard cameras and odometry are used. Ample experimental results with ground truthing from laser scanners demonstrate the accuracy and feasibility of the proposed vision-based cooperative simultaneous localization and tracking algorithm.**

I. INTRODUCTION

Localization is one of the most essential capabilities of autonomous robots [2]. In the single robot localization problem, the location of the robot is inferred based on motion controls and measurements of relative information between the robot and a given map. By properly modeling the uncertainty of the motion commands and the measurements, the robot pose can be estimated in a probabilistic manner [10], [6]. In the multiple robot scenario, the state estimates can be refined through the assistance of other robots. With the ability to detect the teammates, the cooperative localization algorithms improve the localization performance by incorporating measurements of relative information among teammate robots [5], [13], [8]. In the scenarios of tracking using multiple robots, both localization and moving entities should be accomplished [3], [14]. It would be critical for autonomous robots to accomplish localization and tracking in dynamic environments.

This work was motivated by the localization and tracking challenges in the RoboCup Standard Platform League (SPL) competitions as illustrated in Fig. 1. There are six robots playing a 3-by-3 soccer game in the field which consists of two goals in different colors and several white field lines. Fig. 2 illustrates the first challenging scenario in which only few map features are observed by a robot near the field boundary. Fig. 3 illustrates the other challenging scenario in which a robot is asked to look at the ball for preparing a kick but not to observe map features. In these two cases, the observations are insufficient to perform accurate robot localization.

This work was partially supported by grants from Taiwan NSC (#99-2221-E-002-192) and the Intel-NTU Connected Context Computing Center.

C.-H. Chang, S.-C. Wang and C.-C. Wang are with the Department of Computer Science and Information Engineering, and the Graduate Institute of Networking and Multimedia, National Taiwan University, Taiwan [alan,neant]@pal.csie.ntu.edu.tw, bobwang@ntu.edu.tw

C.-H. Chang and S.-C. Wang contributed equally to this work.

(a) RoboCup Standard Platform League

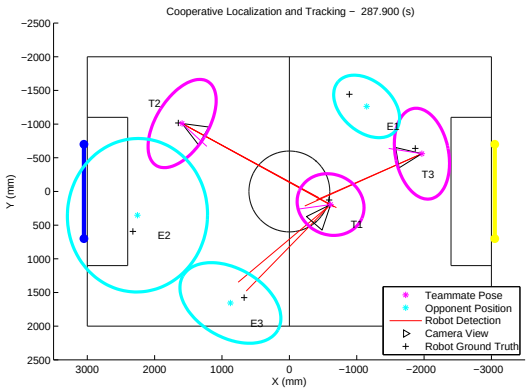

(b) The result of the proposed approach.

Fig. 1. Cooperative simultaneous localization and tracking for the RoboCup Standard Platform League competitions. In (b), the estimated poses and the uncertainties of the teammate robots are shown in magenta ellipses and the opponents in cyan. By fusing the relative measurements (red lines) among the teammates and the opponents, states of all the robots are estimated simultaneously in the proposed approach.

The state-of-the-art cooperative localization approaches may improve localization performance in these two challenging scenarios. In this paper, we will demonstrate that the proposed cooperative simultaneous localization and tracking approach is superior to the cooperative localization approaches. In other words, moving object tracking does contribute to localization. Based on the theoretical framework of simultaneous localization, mapping and moving object tracking [17], an Extended Kalman filter (EKF) is used to accomplish the task in which the poses of the teammate robots and all moving objects are augmented into one state vector. The proposed approach can model the dynamics of the teammate robots and the moving objects in one coherent framework. Three types of measurements are aggregated: (1) relative information between the teammate robots and the map (robot-to-map), (2) relative information between two teammate robots (robot-to-robot), and (3) relative informa-

Fig. 2. The Boundary Case: the robot indicated by the red rectangle detects only one field line and two corners. The bottom images are a sequence of images captured during a right to left head motion (in 2 seconds).

Fig. 3. The Ball Gazing Case: the robot indicated by the red rectangle only detects the ball without any map feature. The bottom images are a sequence of images captured during the task.

tion between teammate robots and moving objects (robot-to-moving-object). All of the pairwise correlations between the teammates and the moving objects are maintained.

The proposed approach is evaluated using the Aldebaran Nao robots in a RoboCup Standard Platform League (SPL) environment. Only onboard cameras and odometry of the robots are used to perform the localization and tracking tasks. Laser scanners are used to collect ground-truth data. The experimental results will demonstrate the effectiveness of the proposed approach in both localization and moving object tracking. In particular, the proposed approach well performs in the difficult cases in which observations are insufficient for self-localization.

The rest of this paper is organized as follows. The next section reviews related works. The front-end image processing modules and their performance are described in Section III. Section IV describes the proposed EKF-based cooperative simultaneous localization and tracking approach. Section V shows the experimental results, and the conclusions are addressed in Section VI.

II. Related Work

For improving self-localization, Fox *et al.* [5] proposed a collaborative localization algorithm based on the histogram filter and the particle filter (PF) to utilize the measurements of relative information between team robots. Based on EKF, Roumeliotis and Bekey [13] proposed augmenting poses of team robots into one state vector and localize all robots simultaneously. Howard et al. [8] formulated the multiple robot localization problem as an optimization problem based on the maximum likelihood criteria. These works extended the localization problem from a single robot to multiple robots.

In the multi-robot simultaneous localization and mapping (SLAM) problem, the single robot SLAM problem is reformulated in which the states of the team robots and the map are estimated concurrently. A number of algorithms based on different filtering techniques have been proposed to solve this problem [9], [16], [4]. In [18], [1], the multi-robot SLAM problem was treated as a map merging problem. However, the environments are assumed to be static in these approaches which could fail in dynamic environments. Given correct moving object detection, the proposed cooperative localization and tracking approach directly deals with the non-static environment by explicitly considering the dynamics of robots and moving objects.

Solving both localization and tracking has been proposed in the literature. In [3], localization is first accomplished using data from laser scanners, and then moving object observations from different robots are shared in which the poses of the robots are assumed to be accurate. Tracking of moving objects is accomplished using multiple EKFs. The correlation between robots and moving objects is not maintained. In [14], localization and tracking are also solved separately. In these works, the mutual benefits of localization and tracking could be limited.

In [7], the relative information between a moving object and a static landmark in one captured image is utilized to track this moving object using a particle filter. Although this approach can theoretically separate localization and tracking as all measurements are related to the map directly, the coexistence of the map features and the moving objects in one image is needed. In [15], a moving object is used to localize and calibrate a sensor network. However, the sensor nodes are stationary.

III. Front-End Image Processing

Recall that three kinds of relative measurements are used in this work. In this section, the front-end image processing modules such as map feature, ball, and robot detection are described as well as the accuracies and uncertainties of the modules. Note that our modules were developed based on the B-Human code release 2009 framework [12], from which the low-level image processing functions such as color segmentation, map feature detection, and ball detection are used in this work.

A. Localization and Tracking in the 2D Space

Although the cameras on the Nao humanoid robots are moving in 3D space, the localization and tracking problems could be reasonably tackled in the 2D space in the RoboCup fields. Given the lowest-center point of an object in an image and the 3D pose of the camera, relative range and bearing of the object in 2D are computed based on the assumption that all the map features and the robots are on the same ground plane.

B. Map Feature and Ball Detection

Map features including point features and line features are extracted for robot self-localization. The goal posts, the center circle, and the corners are three different types of point features. The detection module returns range and bearing measurements of point features. The range accuracy, the angle accuracy, and the maximum sensing range of each kind of features are shown in Table I. Note that the range accuracy and the angle accuracy of the line features are compared in the Hesse normal form. For localization, the center circle and the goal posts are preferred as these features can be easily identified and the measurements are relatively accurate.

TABLE I

STANDARD DEVIATION AND MAXIMUM SENSING RANGE OF MAP FEATURES

	Goal	Center Circle	Corner	Line
σ_{range}(cm)	33.68	18.75	42.45	96.56
σ_{angle}(degree)	11.92	2.49	18.88	41.99
max range(cm)	600	300	300	300

The performance of the ball detection is shown in Table II. The standard deviation of the range increases as the ball becomes farther. The recall rate (the number of the true positives reported by the detection module divided by the number of positives recognized by human) decreases oppositely. The maximum sensing range of the ball detection is about 400 centimeters. The precision is nearly 1 because of the unique color and shape of the ball in the field.

TABLE II

STANDARD DEVIATION AND RECALL OF BALL DETECTION IN DIFFERENT RANGES

	75cm	225cm	375cm	450cm
σ_{range}(cm)	13.09	20.96	32.56	-
σ_{angle}(degree)	4.31	2.94	3.17	-
recall	0.973	0.623	0.076	0.0

C. Nao Robot Detection

The Nao robot detection is the basis of the robot-to-robot and robot-to-moving-object measurements. Our Nao robot detection module works as follows: First, the parts above the field border are removed as depicted in Fig. 4. Second, based on the color segmentation module in [12], the pixels sampled from non-line white segments are clustered. The extracted clusters are classified as Nao robots if the following three criterions are satisfied: (1) the number of segments in the cluster should be larger than 3, (2) the width-to-height ratio should be larger than 0.2, and (3) the highest point of the cluster should be close enough to the border line within 10 pixels as the observed robot should intersect with the field border in the camera view if both of the observing and observed robots are standing in the field. Fig. 4 illustrates a Nao robot detection example. The relative range and bearing can be computed as mentioned in Subsection III-A.

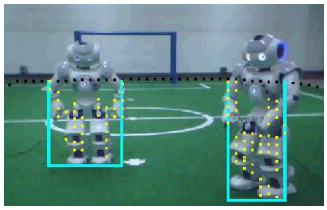

Fig. 4. The robot detection results are plotted on the image as indicated by cyan lines. Black dashed line indicates the field border and yellow dots indicate pixels sampled from non-line white segments.

TABLE III

STANDARD DEVIATION OF ROBOT DETECTION IN DIFFERENT RANGES

	100cm	150cm	200cm	250cm	300cm
σ_{range}(cm)	27.32	31.77	37.91	41.92	65.82
σ_{angle}(degree)	7.95	7.13	6.80	7.28	8.17

The performance of the Nao robot detection module is summarized in Table III and Fig. 5. The recall rate is higher when the target is in the front view than it is in the side view or the back view. The samples of the observations from different views are shown in Fig. 6. In average, the recall rate is above 0.6 within 2 meters and it decreases as the target gets farther. The range accuracy is around 30 centimeters when the target is nearer than 2 meters but grows to around 60 centimeters as the target gets farther. The bearing accuracy is around 7.5 degree. The overall precision is 0.92 where the false positives are mainly arising from the misclassifications of the field lines.

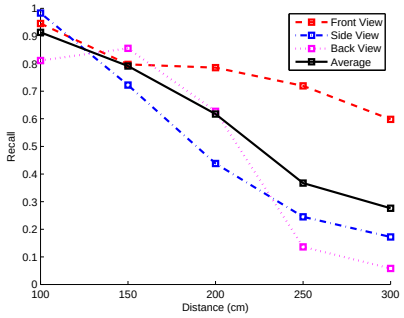

Fig. 5. Recall rates of the proposed robot detection module in different robot views and at different distances.

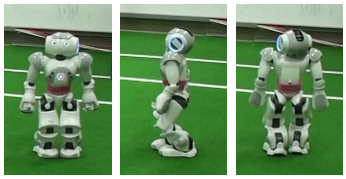

(a) Front (b) Side (c) Back

Fig. 6. Photos of different views of the Nao robot.

IV. Cooperative Localization and Tracking

Thus far, the materials for building the measurement models of the whole system are provided. In this section, the theoretical formulation of the proposed approach is addressed.

A. Augmented State EKF

In order to simultaneously estimate the states of both robots and moving objects in one coherent framework, we augment them all into the state vector X_t:

$$X_t = \left[\begin{array}{cccccc} (R_t^1)^T & \dots & (R_t^N)^T & (O_t^1)^T & \dots & (O_t^M)^T \end{array} \right]^T$$

where t denotes the time index, N denotes the number of robots, M denotes the number of moving objects, R_t^i is the pose of the i^{th} robot at time t, and O_t^j contains the position and velocity of the j^{th} moving object at time t.

B. The Process Model

For teammate robots, the odometry motion model is used. For moving objects, as there is no odometry information, we apply the multiple model tracking approach to account for the unknown motion mode uncertainty. The GPB-1 algorithm [11] combining the constant velocity (CV) model and the stationary model is used to model moving objects.

With the assumption that the motion of robots and tracking objects are all independent, the propagation matrix of the whole system can be written as $G_t = diag(G_{R_t}^1, \dots, G_{R_t}^N, G_{O_t}^1, \dots, G_{O_t}^M)$, where $G_{R_t}^i$ and $G_{O_t}^j$ are the Jacobian matrices of the motion models of the i^{th} robot and the j^{th} moving object respectively. The mean and covariance of the state after the prediction stage at time t can be calculated through the standard EKF procedure.

C. Data Association

Before updating with the incoming measurements, the data associations must be established first. Here, we apply the maximum likelihood data association algorithm with a threshold gating on the Mahalanobis distance between the incoming measurement and the expected measurement. Then the state is updated according to the three sensor models defined in the following subsection.

D. The Sensor Model

In the case that the i^{th} robot detects a moving object and associates it with the j^{th} moving object, the sensor model for robot-to-moving-object measurements is computed as:

$$z_{R_i}^{O_j} = h_{RO}(R_t^i, O_t^j) + \Sigma_{RO_t}.$$

where $h_{RO}(\cdot)$ is a function that transforms the expected j^{th} moving object position in the global coordinate system to the local coordinate system of the i^{th} robot. The Jacobian matrix of this function is

$$\frac{\partial h_{RO}(\bar{R}_t^i, \bar{O}_t^j)}{\partial \bar{X}_t}$$

$$= \left[\begin{array}{ccccccccccc} 0 & \dots & 0 & H_{RO_t}^i & 0 & \dots & 0 & H_{RO_t}^j & 0 & \dots & 0 \end{array} \right]$$

with

$$H_{RO_t}^i = \frac{\partial h(\bar{R}_t^i, \bar{O}_t^j)}{\partial \bar{R}_t^i}$$

and

$$H_{RO_t}^j = \frac{\partial h(\bar{R}_t^i, \bar{O}_t^j)}{\partial \bar{O}_t^j}$$

where $H_{RO_t}^i$ is the i^{th} and $H_{RO_t}^j$ is the $(M+j)^{th}$ element of the matrix.

For the other two types of measurements, the measurement function and the Jacobian matrix can also be defined similarly. The state vector and the covariance matrix can be updated with new retrieved measurements following the standard EKF procedure.

E. Track Management

It is necessary to infer the existences of the moving objects as the tracks of moving objects should be initialized when new ones have been detected and should be pruned when they have not been observed for a long time. Let E_t^i be a binary random variable indicating the existence of the i^{th} track at time t. Then $p(E_t^i|z_{1:t})$ can be estimated recursively with the use of the log odd ratio:

$$\begin{aligned} l_t^i &= \log \frac{p(E_t^i|z_{1:t})}{1 - p(E_t^i|z_{1:t})} \\ &= l_{t-1} + \log \frac{p(E_t^i|z_t)}{1 - p(E_t^i|z_t)} + \log \frac{p(E_t^i)}{1 - p(E_t^i)} \end{aligned}$$

In our implementation, $p(E_t^i|z_t)$ and $p(E_t^i)$ are defined as:

$$p(E_t^i|z_t) = \begin{cases} \sigma, & \text{if } O_t^i \text{ is observed (associated) in } z_t \\ 0.5, & \text{otherwise} \end{cases},$$

and

$$p(E_t^i) = \eta,$$

where σ ($= 0.9$) and η ($= 0.4$) are experimentally determined parameters.

V. Experimental Result

In this section, the ground truth system and the performance of the proposed approach in the general and two challenging situations are described.

A. Ground Truth System

Two SICK LMS 100 laser scanners and one Hokuyo URG-04LX laser scanner are placed around the field to provide the position ground truth of the robots and the ball. The setting of these laser scanners is shown in Fig. 7. The angular sensing ranges of SICK and Hokuyo laser scanners are 270 degrees and 240 degrees respectively. The distance sensing range of the SICK laser scanner is over 40 meters, which is sufficient to cover the whole field. As the height of the ball is low, the Hokuyo laser scanner is used to provide the ground truth of the ball locations. The ball was placed or moved in the 4-meter sensing range of the Hokuyo laser scanner in our experiments.

The data collected from these three laser scanners are clustered and the mean positions of the clustered laser points

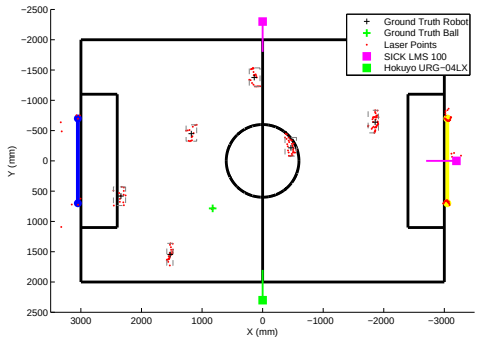

Fig. 7. Filled squares indicate the poses of the laser scanners. The ground truth positions are shown in crosses.

are viewed as the candidates of the ground truth locations of the robots or the ball. These candidates are then associated with the closest estimates and the incorrect associations are re-labeled manually.

B. The General Case

A general case with three teammates and three opponents was tested. The setting is illustrated in Fig. 8 in which the moving patterns of T1, T2, E1, and E2 are indicated by the black dashed arrows. T3 and E3 stayed standing imitating the keepers in the soccer games.

Table IV summarizes the position errors and uncertainties estimated using four different algorithms, including single robot PF-based localization (S-PF), single robot EKF-based localization (S-EKF), cooperative EKF-based localization (CL), and the proposed cooperative EKF-based localization and tracking algorithm (CLAT). The accuracy of the proposed cooperative localization and tracking algorithm outperforms the single robot localization algorithm and is better than the cooperative localization algorithm.

In this case, incorporating moving object tracking slightly improves the result as the single robot localization algorithms have already achieved 13.95 cm accuracy. However, the proposed algorithm not only achieves accurate localization but also provides moving object information at the accuracy around 30 cm and the recall rate 0.78. Table V compares the tracking performance between the EKF-based tracking algorithm by each robot and the proposed cooperative localization and tracking algorithm, which shows that the proposed approach is superior in terms of accuracy and recall.

In the following two cases where the performance of single robot localization degenerates due to insufficient environmental information, our approach exhibits more significant improvements.

TABLE IV
EVALUATION OF THE GENERAL CASE

(a) Position Error (cm)

	T1	T2	T3	Average
S-PF	26.99	28.22	12.26	23.25
S-EKF	8.63	15.05	16.82	13.95
CL	9.12	11.19	16.71	12.75
CLAT	9.19	11.40	16.44	12.71

(b) Uncertainty (cm)

		T1	T2	T3	Average
σ_x	S-EKF	22.55	34.25	23.93	27.41
	CL	19.90	29.53	22.89	24.44
	CLAT	19.61	29.17	22.45	24.08
σ_y	S-EKF	23.03	37.66	34.46	32.33
	CL	20.95	32.43	32.43	29.11
	CLAT	20.78	31.76	31.96	28.65

TABLE V
GENERAL CASE TRACKING EVALUATION

	EKF T1	EKF T2	EKF T3	CLAT
Position Error	28.74	35.08	36.44	31.51
Recall	0.37	0.28	0.34	0.78

C. The Boundary Case

This experiment constructed the boundary case as illustrated in Fig. 9. There were four robots, three teammates in magenta and one opponent in cyan, moving as the black dashed arrows indicated. In order to simulate the data deficiency situation, the behavior of T2 was designed purposely so that its body always faced outside the field and only few map features were observed. An opponent was in front of T2 and two teammates were nearby.

The evaluation results on T2 are summarized in Table VI. For T2, single robot localization achieves the accuracy of 20 cm. Cooperative localization outperforms the single robot localization by 5.7 cm with the use of the robot-to-robot measurements among teammates. By incorporating

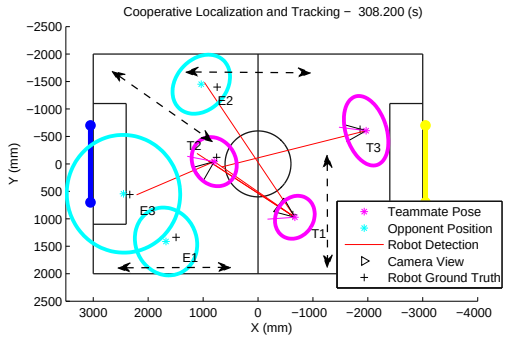

Fig. 8. The general 3-by-3 case. The behaviors of the robots are illustrated by dashed arrows. The estimates and the 2σ uncertainty bounds of the estimates are shown.

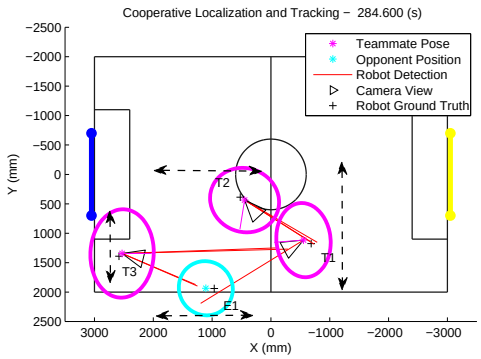

Fig. 9. The boundary case experiment setting illustration.

the moving object tracking, cooperative localization and tracking further improves the accuracy by 4 cm compared with cooperative localization.

TABLE VI
BOUNDARY CASE EVALUATION ON T2

(a) Position Error (cm)

S-PF	S-EKF	CL	CLAT
34.43	20.47	14.82	10.78

(b) Uncertainty (cm)

	σ_x	σ_y
S-EKF	14.13	12.06
CL	13.10	11.32
CLAT	13.00	11.19

D. The Ball Gazing Case

The ball gazing case was tested as illustrated in Fig. 10. A ball was put in the field and the behavior of T2 was designed that it only gazed at the ball and approached the ball once the ball had been detected. The challenge here is that almost no map feature is observable for self-localization when the gaze of the robot is fixed on the ball.

Localization results of different algorithms are shown in Table VII. For T2, with insufficient robot-to-map measurements, self-localization could only rely on the odometry and thus the performance degenerates. Through cooperative localization, the accuracy is improved from 73.54 cm to 20.11 cm. By incorporating moving object tracking, cooperative localization and tracking further improves the accuracy to 12.21 cm.

TABLE VII
EVALUATION OF THE BALL GAZING CASE

(a) Position Error (cm)

	T2	Average
PF	105.35	62.59
EKF	73.54	45.00
CL	20.11	19.59
CLAT	12.21	14.96

(b) Uncertainty (cm)

		T2	Average
σ_x	EKF	66.06	41.60
	CL	22.73	20.01
	CLAT	19.75	18.01
σ_y	EKF	149.81	88.70
	CL	23.43	22.63
	CLAT	19.06	20.48

Fig. 11 shows the results of the EKF-based single robot localization algorithm, the EKF-based cooperative localization algorithm, and the proposed cooperative localization and tracking algorithm. The ball was detected at the first

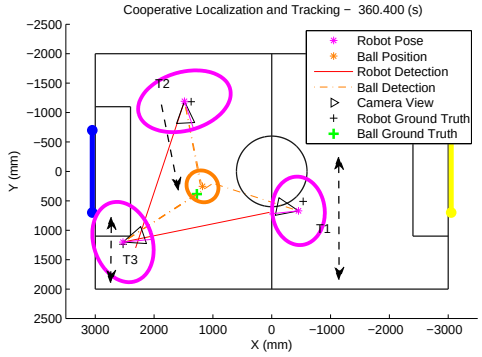

Fig. 10. The ball gazing case experiment setting illustration.

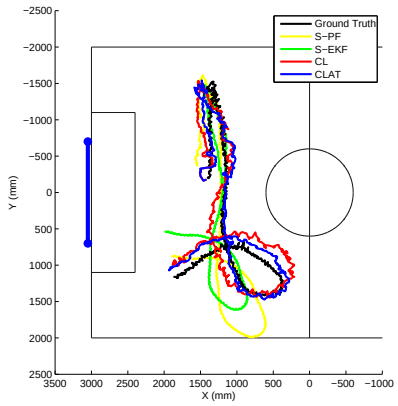

Fig. 12. Trajectory estimates using different algorithms in the ball gazing case. The ground truth is shown in black. The trajectory estimated by EKF self-localization is shown in green, PF-based self-localization in yellow, cooperative localization in red, and cooperative localization and tracking in blue.

time step and the robot started to gaze at and move toward the ball. It can be seen that the position error and the corresponding uncertainty estimated by the EKF-based single robot localization algorithm grows continuously as there is no map feature measurement. The position estimates of the cooperative localization algorithm were close to the ground truth via the assistance from the teammates. The proposed cooperative localization and tracking algorithm achieves more accurate localization through the commonly tracked ball. The estimated trajectories from different approaches are shown in Fig. 12.

VI. CONCLUSION AND FUTURE WORK

In this paper, we have demonstrated that the proposed cooperative simultaneous localization and tracking approach is superior to the state-of-the-art localization approaches. It is shown that augmenting moving objects into the state vector can further improve the performance of EKF-based cooperative localization. The proposed approach was evaluated using the Nao robots in the RoboCup environment with ground truthing from the laser scanners. Only uncertain data from the onboard cameras and odometry were used to accomplish localization and tracking in the challenging scenarios. It is in our interests to develop active localization and tracking, and to investigate the feasibility of distributed localization and tracking.

REFERENCES

[1] A. Birk and S. Carpin, "Merging occupancy grid maps from multiple robots," *Proceedings of the IEEE: Special Issue on Multi-Robot Systems,*, vol. 94, no. 7, pp. 1384 –1397, jul. 2006.

[2] I. J. Cox and G. T. Wilfong, Eds., *Autonomous robot vehicles*. Springer-Verlag New York, Inc., 1990.

[3] M. Dietl, J.-S. Gutmann, and B. Nebel, "Cooperative sensing in dynamic environments," in *IEEE/RSJ International Conference on Intelligent Robots and Systems*, vol. 3, 2001, pp. 1706–1713 vol.3.

[4] J. Fenwick, P. Newman, and J. Leonard, "Cooperative concurrent mapping and localization," in *IEEE International Conference on Robotics and Automation, 2002*, vol. 2, 2002, pp. 1810 – 1817 vol.2.

[5] D. Fox, W. Burgard, H. Kruppa, and S. Thrun, "A probabilistic approach to collaborative multi-robot localization," *Autonomous Robots*, vol. 8, no. 3, pp. 325–344, 2000.

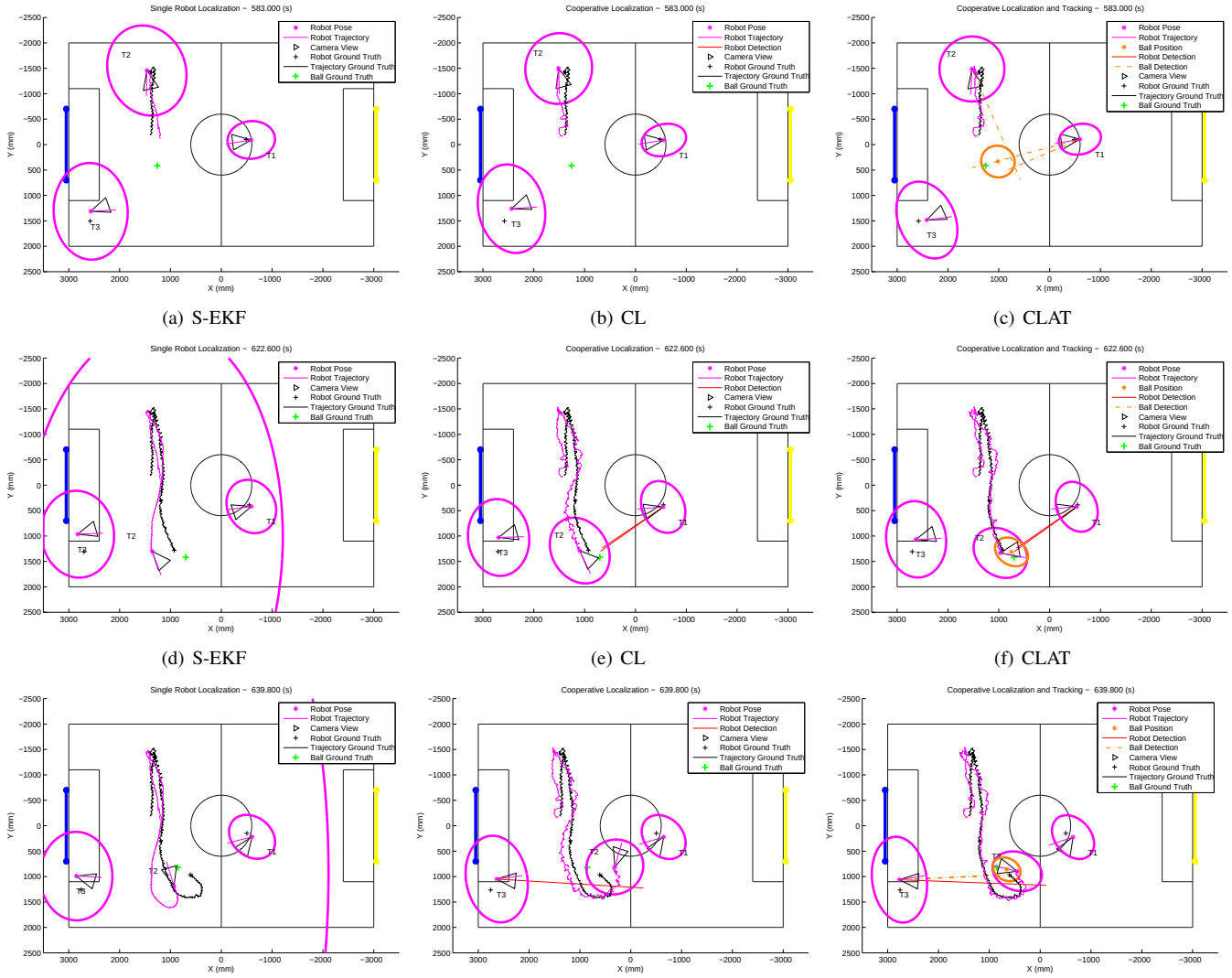

(a) S-EKF (b) CL (c) CLAT

(d) S-EKF (e) CL (f) CLAT

(g) S-EKF (h) CL (i) CLAT

Fig. 11. The results of the ball gazing case using different algorithms. In the S-EKF approach, the uncertainty bound of the robot T2 grows gradually as there are odometry data only. In the CL approach, the localization performance is improved by adding teammate-to-teammate information. In the proposed CLAT approach, the result is further improved. The robot heading estimates are also improved by the proposed CLAT approach.

[6] D. Fox, W. Burgard, and S. Thrun, "Markov localization for mobile robots in dynamic environments," *Journal of Artificial Intelligence Research*, vol. 11, pp. 391–427, 1999.

[7] D. Gohring and H.-D. Burkhard, "Multi robot object tracking and self localization using visual percept relations," in *IEEE/RSJ International Conference on Intelligent Robots and Systems*, oct. 2006, pp. 31–36.

[8] A. Howard, M. Matark, and G. Sukhatme, "Localization for mobile robot teams using maximum likelihood estimation," in *IEEE/RSJ International Conference on Intelligent Robots and Systems*, vol. 1, 2002, pp. 434–439.

[9] A. Howard, "Multi-robot simultaneous localization and mapping using particle filters," *International Journal of Robotics Research*, vol. 25, no. 12, pp. 1243–1256, 2006.

[10] J. Leonard and H. Durrant-Whyte, "Mobile robot localization by tracking geometric beacons," *IEEE Transactions on Robotics and Automation*, vol. 7, no. 3, pp. 376–382, June 1991.

[11] X. R. Li and V. P. Jilkov, "Survey of maneuvering target tracking. part v. multiple-model methods," *IEEE Transactions on Aerospace and Electronic Systems*, vol. 41, no. 4, pp. 1255– 1321, October 2005.

[12] T. Röfer, T. Laue, J. Müller, O. Bösche, A. Burchardt, E. Damrose, K. Gillmann, C. Graf, T. J. de Haas, A. Härtl, A. Rieskamp, A. Schreck, I. Sieverdingbeck, and J.-H. Worch, "B-human team report and code release 2009," 2009, only available online: http://www.b-human.de/download.php?file=coderelease09_doc.

[13] S. Roumeliotis and G. Bekey, "Distributed multirobot localization," *IEEE Transactions on Robotics and Automation*, vol. 18, no. 5, pp. 781–795, oct. 2002.

[14] T. Schmitt, R. Hanek, S. Buck, M. Beetz, and T. S. R. Hanek, "Cooperative probabilistic state estimation for vision-based autonomous mobile robots," *IEEE Transactions on Robotics and Automation*, vol. 18, pp. 670–684, 2001.

[15] C. Taylor, A. Rahimi, J. Bachrach, H. Shrobe, and A. Grue, "Simultaneous localization, calibration, and tracking in an ad hoc sensor network," in *The Fifth International Conference on Information Processing in Sensor Networks*, 2006, pp. 27–33.

[16] S. Thrun and Y. Liu, "Multi-robot slam with sparse extended information filers," *Robotics Research*, vol. 15, pp. 254–266, 2005.

[17] C.-C. Wang, C. Thorpe, S. Thrun, M. Hebert, and H. Durrant-Whyte, "Simultaneous localization, mapping and moving object tracking," *The International Journal of Robotics Research*, vol. 26, no. 9, pp. 889–916, September 2007.

[18] X. Zhou and S. Roumeliotis, "Multi-robot slam with unknown initial correspondence: The robot rendezvous case," in *IEEE/RSJ International Conference on Intelligent Robots and Systems*, oct. 2006, pp. 1785–1792.